View Article Online / Journal Homepage / Table of Contents for this issue

Strain induced clustering in polyelectrolyte hydrogels†

Guillaume Miquelard-Garnier, Costantino Creton* and Dominique Hourdet*

Received 12th November 2007, Accepted 6th February 2008
First published as an Advance Article on the web 13th March 2008
DOI: 10.1039/b717460h

Published on 13 March 2008. Downloaded by Arts et Metiers Paris Tech on 29/06/2016 15:33:22.

Systematic large strain compression measurements have been performed on polyelectrolyte hydrogels based on modified PAA crosslinked by bifunctional thiols. For compressive strains larger than a critical value depending on polymer concentration, we observed a significant hysteresis, strain-hardening and a stress plateau during unloading. This was attributed to strain-induced ionic clustering due to electrostatic interactions that can become attractive if chains are close enough to each other. This phenomenon is dynamic and reversible but a long lifetime for the clusters has been identified. Although clustering between like-charge chains has been reported for hydrogels, it is the first time that this phenomenon is caused by deformation. This effect is potentially important as we strive to understand the behaviour of all polyelectrolyte hydrogels at large strains which are highly relevant for fracture properties.

Introduction

Polyelectrolytes are among the most studied macromolecular systems since the early works of Katchalsky *et al.*[1] in the 50's. They are of fundamental importance since most biological systems are, in fact, polyelectrolytes,[2] DNA being the most famous one.

However, several experimental results remain poorly described theoretically. Compared to neutral polymers, the ionisable groups and the counterions create long-range forces (Coulomb type) in the system. In consequence, both long-range and short-range (excluded volume) interactions are present, leading to much more complex systems than for the neutral polymers.[3]

One of the most astonishing behaviours in polyelectrolyte solutions is the attraction that can occur between macroions. In principle it is counterintuitive to think of attractive interactions between polymers carrying charges with the same sign.

Biologists working on DNA have reported quite a long time ago *in vitro* condensation of DNA by multivalent cations leading to toroidal bundles of concentrated DNA.[4,5] Since then, many studies have appeared, reporting condensation or clustering of chains also for a wide range of synthetic polyelectrolytes and experimental conditions.[6–10]

Basically, attraction between two chains of the same charge has been explained by Oosawa[11] 35 years ago, using the counterion condensation mechanism introduced by Manning.[12] When the polyelectrolyte is strongly charged, the electrostatic potential on the chain is large and in consequence some of the counterions remain "bound" to the chain. This leads to an effective charge for the chain inferior to its "real" one. However, the condensed counterions are not motionless: they can move freely along the chain, and create some fluctuations in the charge density of the chain. When two chains are close enough, a charge fluctuation in the first chain polarizes the second chain and creates a fluctuation of opposite charge. The Coulomb interaction between these charge fluctuations leads to an attractive force between the two chains. Oosawa estimated this force for two rods, using the Debye–Hückel approximation, as a function of the distance between the two chains and compared it to the repulsive force due to the electrostatic interactions.

He showed that for small distances of the order of the Bjerrum length, the attractive interaction is dominant. A lot of more complex models have been presented since,[13–16] but to the best of our knowledge, none of them take into account all the parameters that seem to have an influence on this phenomenon (valence of the counterion, charge density on the chain, chain flexibility and even chain end effect).[17]

Some additional effects due to the charges have been reported in polyelectrolyte hydrogels: the well-known increased swelling ratio, caused by the osmotic pressure induced by the counterions, has been the focus of many studies.[18–20] The influence of the charges on the elastic modulus of the gel was also investigated both experimentally and theoretically.[21–23] More recently, ion binding processes have been observed for strongly charged polyelectrolytes, affecting the swelling and potentially affecting the modulus (by creating additional crosslinks in the case of multivalent cations) and even leading to a gel collapse.[24–26]

More generally, polyelectrolyte hydrogels are widely used in life sciences (drug delivery, artificial cartilage, contact lenses), food science and engineering (superabsorbants, microfluidics)[27,28] and the understanding of their macroscopic mechanical properties remains an important challenge.

For all hydrogels, less attention has been paid to their large strain properties (non Gaussian elasticity regime and fracture), because they were usually considered as weak materials.[29] However, newly developed hydrogels displaying truly amazing mechanical properties (modulus, extensibility…)[30,31] have sparked a renewed interest for studying systematically and understanding these large strain properties.[31–33]

Physico-chimie des Polymères et des Milieux Dispersés, UMR 7615, UPMC-CNRS-ESPCI, 10 rue Vauquelin, 75005 Paris, France. E-mail: costantino.creton@espci.fr; dominique.hourdet@espci.fr; Fax: +33 (0)1 40 79 46 86; Tel: +33 (0)1 40 79 46 43

† Electronic supplementary information (ESI) available: Elements of polyelectrolyte scaling theory, figures showing polyelectrolyte chains in dilute and semidilute solution. See DOI: 10.1039/b717460h

This journal is © The Royal Society of Chemistry 2008

View Article Online

Published on 13 March 2008. Downloaded by Arts et Metiers Paris Tech on 29/06/2016 15:33:22.

In this paper we focused on the behaviour of model polyelectrolyte hydrogels using compression tests at large strains and compared their behaviour with that of neutral elastic networks of flexible chains. We demonstrate a strain induced aggregation mechanism due to the attractive interaction between like charges and present some hypotheses for this mechanism.

Experimental part

The synthesis of the polymer precursors and hydrogels was described in details in our preceding paper[34] and we only summarize the most important steps.

Materials

Polymer precursor. Poly(acrylic acid) (PAA) was obtained in its acid form from Aldrich. Its number average molecular weight as characterized by size exclusion chromatography (SEC) was $M_n = 35$ kg mol^{-1} ($M_w/M_n = 10$).

Modification of PAA precursor. PAA chains were modified by introducing a given proportion of double bonds (allylamine) along the backbone, in order to crosslink the chains afterwards. The reaction was carried out in an organic solvent (*N*-methyl-2-pyrrolidone, later referred to as NMP) at 60 °C by grafting amino terminated molecules (allylamine) onto the carboxylic acids of the polyacrylic backbone in the presence of dicyclohexylcarbodiimide (DCCI) which activates the formation of the amide bond. 10 mol% double bonds were introduced along the backbone following this quantitative and statistical reaction and the resulting polymer, obtained in its sodium salt form (PAANa) after precipitation with a NaOH excess, will be referred to as PAA10db.

Synthesis of the hydrogels. The reaction was carried out in water, at room temperature and under atmospheric conditions. Modified PAA, dithioerythritol (bifunctional thiol) and KPS (potassium peroxodisulfate) were separately dissolved in water at the desired concentration (KPS and dithioerythritol are always used in stoichiometric proportions relative to the initial number of double bonds added). All concentrations, for solutions and gels, are expressed in % w/w.

The KPS was then added to the PAA solution under stirring and finally dithioerythritol was quickly added into the solution. After an energetic stirring during a few seconds, the solution was finally left to rest for gelation. As the pH of a solution of modified PAANa is around 7 in our range of concentrations and the pK_a of acrylic acid is 4.2, the proportion of charged monomers along the backbone is close to 1.

The gels were always prepared and mechanically tested at their preparation concentration varying from 5 to 8%, far from the equilibrium swelling (for a 6% hydrogel, the swelling ratio is $Q \approx 16$ whereas at equilibrium $Q_e \approx 90$). At these concentrations, entanglement effects are negligible.[34]

Complementary experiments were performed in salted water using the same preparation method for the hydrogels: instead of dissolving the PAA in pure water, it was dissolved in a NaCl solution. Two concentrations of NaCl were used (5 mol L^{-1} and 0.2 mol L^{-1}), so that in one case the ratio polymer charges : salt charges was roughly 1 : 5 and in the other case 5 : 1.

Mechanical tests

The experiments were performed on a custom designed mechanical tester[35] with a force resolution of 0.01 N and a displacement resolution of 0.1 μm, which is adapted to the testing of small and soft samples. The apparatus is displacement controlled but the compression of the gel sample is stopped when a preset value of the compressive force is attained. At that stage the displacement is either kept constant (for relaxation tests) or ramped back to zero (for the standard compression–decompression tests). The displacement rate (crosshead velocity) is always kept the same for the compression and decompression part of the experiment.

Preparation of the samples. A fixed amount of polymer solution was cast in a cylindrical PDMS mould (diameter $d_0 = 5.4$ mm) for each sample in order to obtain cylinders with identical heights after crosslinking. The solution was then left to react and gelify during one night. To prevent the sample from drying, the mould was put between two glass slides in a closed and humidified chamber.

For the experiments performed with the same polymers in organic solvents, the process is slightly different. The gels were prepared in water first as described before. The poly(acrylic acid) was then converted to its acid form by deswelling it gently in an excess of HCl solution at 0.01 mol L^{-1}, and after that in a HCl solution at 0.05 mol L^{-1} to prevent any shape modifications or macroscopic fractures in the gel if it is deswelled at a too high acid concentration due to the osmotic pressure. After several rinses with ethanol to eliminate the NaCl salt formed, the gel was then dried slowly at room temperature (the drying was controlled by sample weighing). When the gel was dry, it was swollen in NMP at the desired concentration. We chose NMP because its density (1.03) is close to that of water and its boiling point is high (202 °C), preventing the gels from drying. PAANa is also insoluble in NMP, ensuring the conversion of the PAA to its acidic form is total: NMP is chosen to prevent any further ionization of the carboxylic groups which could happen if the uncharged gel was swollen in water, following the self-dissociation equilibrium:

$$RCOOH + H_2O \rightleftarrows RCOO^- + H_3O^+ \quad (pK_a = 4.2)$$

To study identical gel structures in both solvents, the molar concentration of polymer was kept constant for both water and NMP (for a chain density equivalent to that of a 6% w/w hydrogel, $Q_{NMP} \approx 20$ and $Q_{e\ NMP} \approx 25$).

Compression measurements. Once the gel cylinder was formed, it was demolded and its height measured precisely. The gel was placed on a glass slide and brought into contact with a second glass surface to a point of maximum compression before being retracted back to zero displacement.

To avoid drying and to obtain frictionless boundary conditions between the gel and the glass slides, dodecane (immiscible with water, $T_{eb} = 216$ °C) was put on the gel top and bottom surfaces and on the glass slides. In the case of NMP gels,

 This journal is © The Royal Society of Chemistry 2008

View Article Online

Published on 13 March 2008. Downloaded by Arts et Metiers Paris Tech on 29/06/2016 15:33:22.

a silicone lubricant was used instead of dodecane to prevent any exchange of solvent in the gel during the experiment. Drying of the gel was verified in the experimental conditions (gel between two glass slides and surrounded by dodecane) and was found to be less than 2% in terms of mass loss for 30 minutes (*i.e.* the mean time for an experiment). For a 3600 s experiment (relaxation experiments), the mass loss was estimated to be around 3%. In consequence, drying is assumed to be a negligible phenomenon in every further analysis.

Load and displacement data were collected during the experiment, and the contact area and shape of the gel were visually monitored *via* a microscope. In this way we could clearly see that slippage occurred at the interface and that the gel deformed at constant macroscopic volume and with an essentially full-slip boundary condition. In these experiments, we performed a uniaxial compression test equivalent to a biaxial deformation in the plane normal to the loading direction. Fig. 1 shows a schematic representation of this test set up.

In this work, a typical compression test consists of an initial compressive contact to −0.03 N to ensure a reproducible starting point of complete contact between the gel and glass surfaces. Below this value, the adhesive forces causing a jump in contact and the lack of parallelism between the probe and the gel caused irreproducibility of the results. This procedure ensured values of the initial gel modulus in quantitative agreement with the rheological measurements obtained with an AR1000 rheometer (see ref. 34) presented in Fig. 2. This is not surprising since the elastic linear regime for these gels lasts for a large range of deformations (less than 5% variation in the G' value for deformations varying from 1 to 100%).

Unfortunately, the non-deformed and small deformations data (λ close to 1) were not collected with this procedure and it is only in a later stage that we realized that these data could be important to interpret more fully the hysteresis.

The test then begins with a compression step performed at a constant crosshead speed (10 μm s^{-1}, 50 μm s^{-1} or 200 μm s^{-1}, corresponding to an initial strain rate of about 0.29×10^{-2} s^{-1}, 1.4×10^{-2} s^{-1}, 5.7×10^{-2} s^{-1} for an initial sample height of 3.5 mm) to a maximum load (varied between 0.5 and 5 N corresponding to true stresses varying from 6.5 kPa to 37 kPa), followed by immediate retraction to zero displacement at the same speed and a wait time (about 1 minute), until the next cycle of compression. Some experiments were also performed at 1 μm s^{-1} and 600 μm s^{-1}.

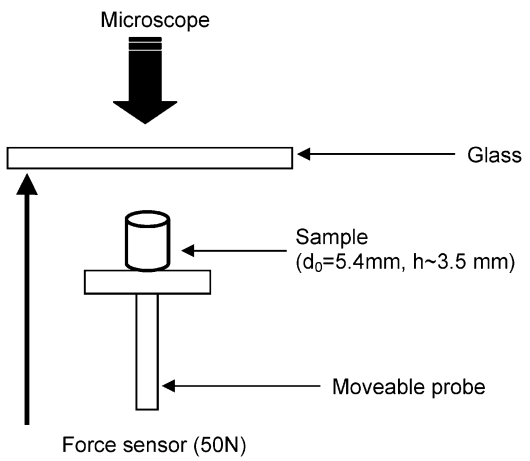

Fig. 1 Schematic representation of the compression test apparatus.

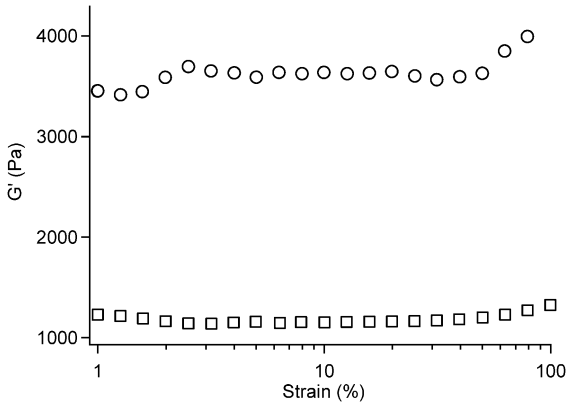

Fig. 2 Plateau modulus for the PAA10db 6% (circles) and 5% (squares) as a function of the strain.

The samples in deformed and undeformed geometry are schematically shown in Fig. 3 and in the following discussion we will use the following parameters to characterize the strain: the compression parameter lambda is defined as $\lambda = h/h_0$, where h_0 is the undeformed height of the gel cylinder and h is its deformed height. Since a uniaxial compression results in an equibiaxial extension in the other two directions, it is sometimes convenient to describe the deformation of the sample in those coordinates. Because of the constraint of deformation at a constant volume the two are simply related by:

$$\lambda_{biax} = \frac{1}{\sqrt{\lambda}} \quad (1)$$

.**Relaxation experiments.** Relaxation experiments were also performed on the same apparatus: the gel was brought into contact with the glass slide to a point of maximum compression at high speed (200 μm s^{-1}, meaning that it took roughly 5 to 10 seconds to bring the gel to its maximum compression). The displacement was then kept constant for a certain time (typically 3600 s), and the gel was left to relax. Force and time data were collected.

Complementary relaxation results were obtained using an ARES rheometer. After gelation directly in the rheometer (as described previously), a 10% deformation was applied to the sample, and the evolution of G' was measured over time.

Results

In Fig. 4, we plotted the true stress defined as $\sigma_{true} = -(F/\pi a_0^2)\lambda$ *versus* λ of a full compression cycle (from 1 to 5 N) for a PAA10db 6% hydrogel, where F is the experimental force and a_0 is the initial radius of the gel cylinder (for convenience, true stress is defined as positive). Using the true stress effectively normalizes the data for the slight differences in the initial height of the samples due to preparation.

Several observations can be made from these results:

1. By fitting the nominal stress $\sigma_{comp} = (F/\pi a_0^2)$ *versus* ε (ε is the deformation of the sample defined as $(h - h_0)/h_0$) in the linear regime (for $\varepsilon > -0.45$), the elastic modulus can be easily obtained, as shown in Fig. 5 (slope of the fitting curve).

View Article Online

Published on 13 March 2008. Downloaded by Arts et Metiers Paris Tech on 29/06/2016 15:33:22.

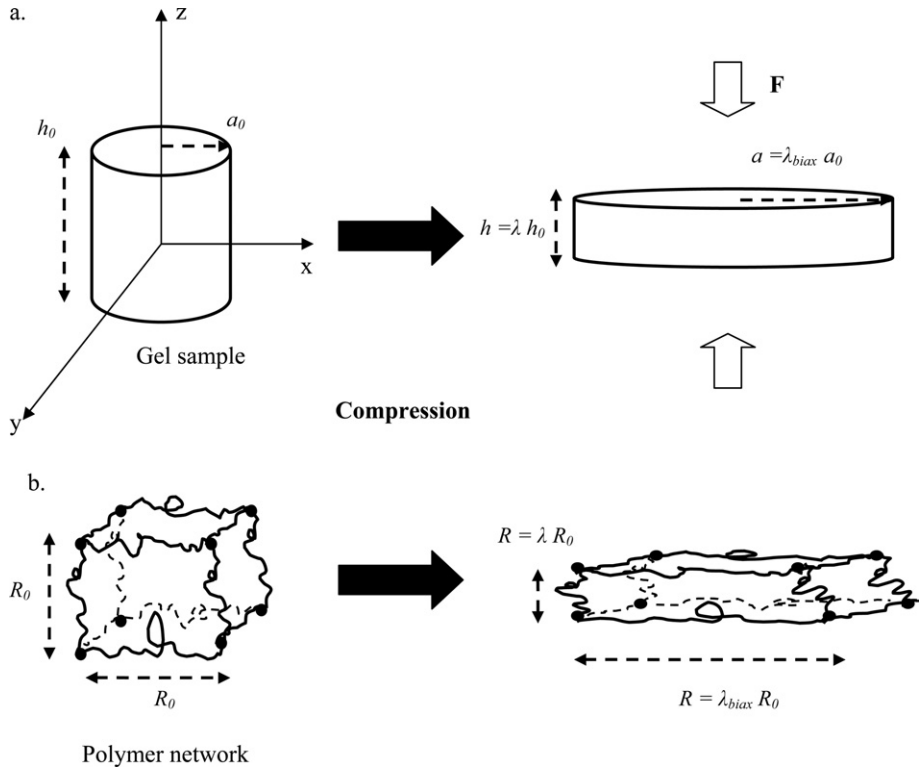

Fig. 3 Schematic representation of a compression test (a) on a gel sample (b) from the molecular point of view (based on an affine deformation).

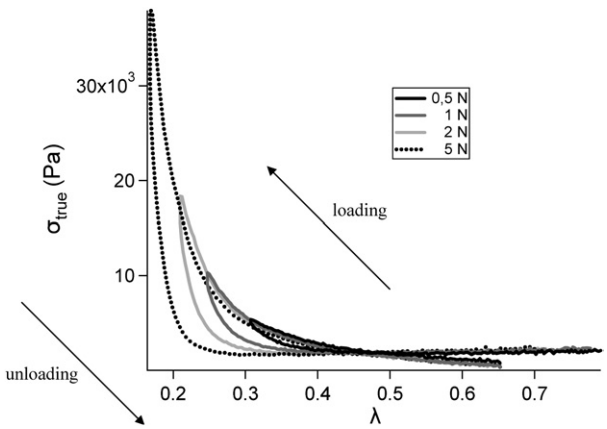

Fig. 4 Compressive stress *vs.* compressive lambda for the same PAA10db sample (6% w/w) with increasing maximum force values (0.5 N, 1 N, 2 N, 5 N).

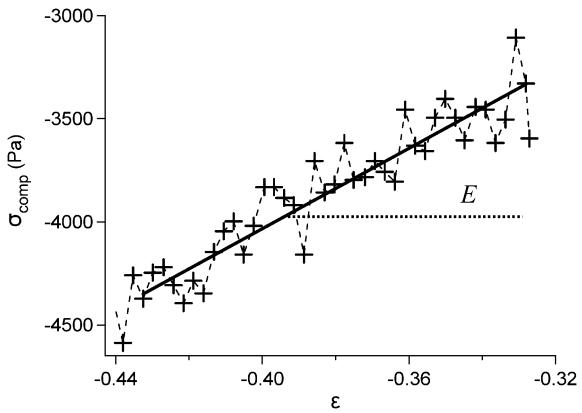

Fig. 5 Determination of the hydrogel's Young's modulus by compression tests on a PAA10db sample at 6%.

For a 6% hydrogel, $E \approx 9500 \pm 500$ Pa. For a Poisson's ratio of $\frac{1}{2}$ (small deformations at constant volume), we have $E = 3G$, which gives a shear modulus $G \approx 3$ kPa. This value is really close to the one obtained by rheological measurements for 6% w/w hydrogels ($G'_{plateau} \approx$ 3000–3500 Pa).[34] This was verified for all concentrations used. The oscillation of the curve of roughly 500 Pa is due to the force resolution of the experimental apparatus ($\triangle F \approx 0.01$ N gives, with $a_0 = 2.7$ mm, $\triangle \sigma \approx 450$ Pa).

2. The perfect superposition in Fig. 4 of the loading curves of tests performed in succession on the same sample demonstrates that there is no irreversible fracture of covalent bonds during the loading and unloading experiments, so the process is fully reproducible.

3. There is a strong strain hardening that appears suddenly and increases very sharply below a certain range of λ (close to 0.3 for a PAA10db 6% hydrogel, see Fig. 4).

4. An important hysteresis appears as a certain deformation is reached ($\lambda \approx 0.3$) and increases with increasing deformation which is surprising for such elastic materials.

5. The unloading curve shows a plateau stress around 2 kPa that lasts for a large range of deformations (λ between 0.3 and 0.7).

These results are very surprising since the gels were purely elastic materials in the small deformation regime (on the order

 This journal is © The Royal Society of Chemistry 2008

View Article Online

Published on 13 March 2008. Downloaded by Arts et Metiers Paris Tech on 29/06/2016 15:33:22.

of 3 orders of magnitude between the G' and the G'' measured in rheology).[34] This behaviour could be due to an inhomogeneous network structure: a percolating structure of short chains between crosslinks would give a stronger hardening than predicted for a homogeneously crosslinked network (since their finite extensibility is lowered), but it is not clear why such a mechanism would give rise to such a hysteresis. We investigated therefore more systematically the effect of the experimental parameters on both the strain hardening and the hysteresis.

Strain hardening and maximum extensibility

Focusing on the strain hardening observed in our tests, we can try to fit the loading curve of the hydrogels quantitatively by using a simple nonlinear elastic constitutive equation which includes this effect. In a relatively recent paper,[36] Gent proposed a simple empirical model for unentangled crosslinked networks undergoing strain hardening at large strains. He proposed the following expression for the elastic strain energy per unit volume:

$$W = -\frac{G}{2} J_m \ln\left(1 - \frac{J_1}{J_m}\right) \quad (2)$$

, where G is the shear modulus, and J_1 is the first stress invariant, which for uniaxial deformation in the 1-direction is given by:

$$J_1 = \lambda_1^2 + 2\lambda_1^{-1} - 3, \quad (3)$$

where λ_1 is the principal stretch ratio in the 1-direction (λ in our tests). In this model J_m is an adjustable parameter representing finite extensibility as a maximum allowable value for the first stress invariant. Since this model is based on the fact that the maximum extensibility is directly correlated to a maximum value of the first stress invariant (independent of the particular choice of coordinates axes), it should be valid for every type of deformation (simple extension, pure shear, simple shear and equibiaxial extension). This has been discussed by several authors.[37,38]

In consequence, the constitutive equation and eqn (1) can be used to predict the true stress[32,36] as a function of λ_{biax} with two adjustable parameters, G and J_m:

$$\sigma_{true} = G \frac{\lambda_{biax}^2 - \lambda_{biax}^{-4}}{[1 - (J_1/J_m)]} \quad (4)$$

The loading curves were fitted for the three types of hydrogels and for polymer concentrations varying from 5 to 8%. The results for the PAA10db hydrogels are presented in Fig. 6 at $v = 50\ \mu m\ s^{-1}$ ($1.4 \times 10^{-2}\ s^{-1}$). The fits are shown as full lines. Since we focused on the strain hardening at large strains, our fits attributed a greater weight to the large strain portion and hence to the J_m parameter. In consequence, to obtain the best fits possible on the large strain portion, the fits were always performed on the loading curves of experiments performed with the maximum load that could be applied without breaking the sample.

Nevertheless the G value obtained from the fits always fell within the range of the experimental small-strain values that were found by rheological measurements, as discussed before. An example is given in Fig. 6 with PAA10db hydrogels where we can see that the Gent equation fits fairly well the strain hardening of our networks. The numerical values are reported in Table 1.

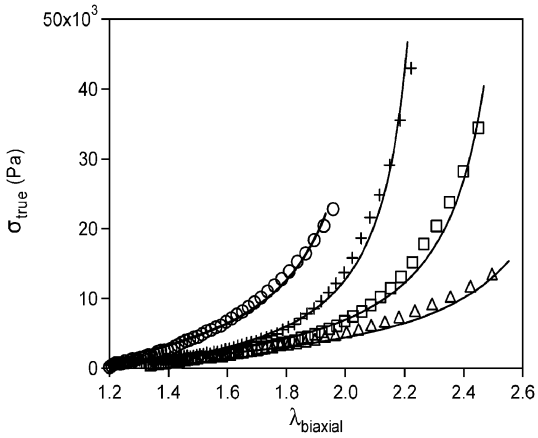

Fig. 6 Loading compressive stress for PAA10db hydrogels at 8% (circles), 7% (crosses), 6% (squares) and 5% (triangles). The Gent fits are in black lines.

Table 1 Theoretical approximation for the maximum extensibility[a]

C	5%	6%	7%	8%
$\lambda_{max,\ e}$	6.7	4.9	4.6	4
$\lambda_{max,\ G} = N_c^{1/2}$	8.9	6.3	5.7	4.7
$\lambda_{max,\ exp}$ (Gent fits), standard deviations obtained from different samples	4.3 ± 0.3	3.7 ± 0.3	3.3 ± 0.2	3.1 ± 0.2
J_m, standard deviations from the Gent fit on a given sample	15.2 ± 0.2	10.1 ± 0.1	7.3 ± 0.05	6.6 ± 0.05

[a] Close results were obtained for $\lambda_{max,\ e}$ and $\lambda_{max,\ G}$ using another literature value for the length of a Kuhn monomer b.[44]

We can see on these graphs that J_m (which is related to the value of λ_{biax} where the curve diverges) increases with decreasing concentration for both gels. The fitted value of J_m gives us access to the maximal experimental value of the first strain invariant. This value can then be used to estimate the maximum value of the extensibility $\lambda_{max,\ exp}$ in uniaxial extension which can be compared to molecular models of chain extension. From eqn (3) we obtain simply

$$J_m = \lambda_{max,\ exp}^2 + 2\lambda_{max,\ exp}^{-1} - 3 \quad (5)$$

which leads to ($\lambda_{max,\ exp}^{-1}$ can be neglected since J_m is on the order of 10):

$$\lambda_{max,exp} \approx \sqrt{J_m + 3} \quad (6)$$

The experiments are in biaxial extension, but to compare the data to the theoretical predictions, we are in fact using the corresponding uniaxial extension value (combining eqn (1) and (5), we obtain that $\lambda_{biax,\ m}$, the maximal biaxial lambda value obtained using the Gent fits, is given by $\lambda_{biax,m} \approx \sqrt{\frac{J_m+3}{2}}$ which leads to $\lambda_{max,\ exp} \approx \sqrt{2}\lambda_{biax,\ m}$. This is in good agreement with experimental studies on rubbers).[39,40]

We can try to compare these experimental results to a theoretical value for the finite extensibility of a single chain based on the

View Article Online

Published on 13 March 2008. Downloaded by Arts et Metiers Paris Tech on 29/06/2016 15:33:22.

theory of polyelectrolytes in solutions and on the molecular theory of rubber elasticity.[41] To calculate a theoretical maximum extensibility for the individual chain, the assumption used is the following: in its maximum stretched state, the size of the chain between two crosslinks is $R_{max} = Nb$ with N the number of Kuhn monomers (referred to in the following as N_c since we are interested in the number of Kuhn monomers between two crosslinks) and b the length of a Kuhn monomer. For a Gaussian chain (this is a first order approximation for a PAA chain dissolved in water), the maximum extensibility λ_{max} is then simply this value divided by the average end-to-end distance of a chain with N_c monomers $\langle R^2 \rangle = N_c^{1/2} b$.

$$\lambda_{max,\,G} = R_{max}/N_c^{1/2} b = N_c^{1/2} \tag{7}$$

However, if the chain is a polyelectrolyte, the effect of charges has to be taken into account as they affect chain conformation. The influence of the charges is concentration dependent, with two distinct regimes. In dilute solutions, polyelectrolytes are almost fully stretched due to strong electrostatic intrachain interactions: they can be seen as stretched electrostatic blobs.[42] In semidilute solutions, the electrostatic interactions are screened by other chains and counterions, and the chains tend toward their Gaussian conformation. This occurs when the electrostatic blobs start to overlap.

In consequence, the two important parameters here are the overlap concentration from dilute to semidilute solutions, c^*, and the concentration at which the electrostatic blobs begin to overlap, c^{**} (concentration at which the concentrated regime begins).[42] c^* is given by:

$$c^* \approx \frac{1}{N_c{}^2 b^3} \tag{8}$$

and in the highly charged limit c^{**} is given by:

$$c^{**} \approx \frac{1}{b^3} \tag{9}$$

Between these two regimes (dilute and "Gaussian" when all the electrostatic interactions are screened), the chain has an intermediate conformation: a random walk of correlation blobs (the correlation length ξ which is the average mesh size of the semidilute solution, see Fig. 7 and ESI†) and the chain size for a strongly charged polyelectrolyte is given[3] by:

$$R_e \approx b^{1/4} c^{-1/4} N_c^{1/2}. \tag{10}$$

To calculate N_c in the gels, we used results from our previous work:[34] titration and rheological measurements gave us the average number of effective crosslinks. To estimate the Kuhn segment length b, we referred to the literature[43] ($b \approx 15.7$ Å). The overlap concentration c^* is then estimated to be close to 0.65×10^{-4} mol L^{-1} $\approx 4 \times 10^{-8}$ Å^{-3} (in terms of Kuhn monomer concentration) and $c^{**} \approx 3 \times 10^{-4}$ Å^{-3}. The Kuhn concentration in our gels is estimated as follows:

$$c_K = \frac{10^3 C_{(w/w)}}{M_{AA10dbNa}\left(1 - C_{(w/w)}\right)} \frac{2}{C_\infty} \text{ mol L}^{-1} \tag{11}$$

where C_∞ is the Flory characteristic ratio for poly(acrylic acid).[43]

The different regimes of chain extension are summarized in Fig. 7: the solutions and gels are clearly in the semidilute regime and the chain conformation should be close to Gaussian.

Coming back to the maximum extensibility $\lambda_{max,\,e}$ for a polyelectrolyte in semidilute solution, using eqn (10), we have:

$$\lambda_{max,e} = \frac{R_{max}}{R_e} = \frac{N_c b}{b^{1/4} c^{-1/4} N_c^{1/2}} = N_c^{1/2} b^{3/4} c^{1/4}. \tag{12}$$

It is important to note that this value for $\lambda_{max,e}$ is the minimum possible value using this model, since we considered the maximum possible value of R_e *i.e.* the case of a fully stretched polyelectrolyte chain in dilute solution.

The values obtained for the theoretical and experimental λ_{max} are summarized in Table 1. The maximum extensibility of a Gaussian chain is presented, and compared to the theoretical value for a fully charged polyelectrolyte in semidilute solution. Additional details on the derivation of these predictions are given in the supplementary material.†

The experimentally measured values of λ_{max} are significantly lower than the theoretically predicted ones regardless of the model used: considering the Gaussian assumption is the upper limit and the highly charged assumption the lower limit, the experimental results should be between the values obtained with these models. This result is surprising since the detailed

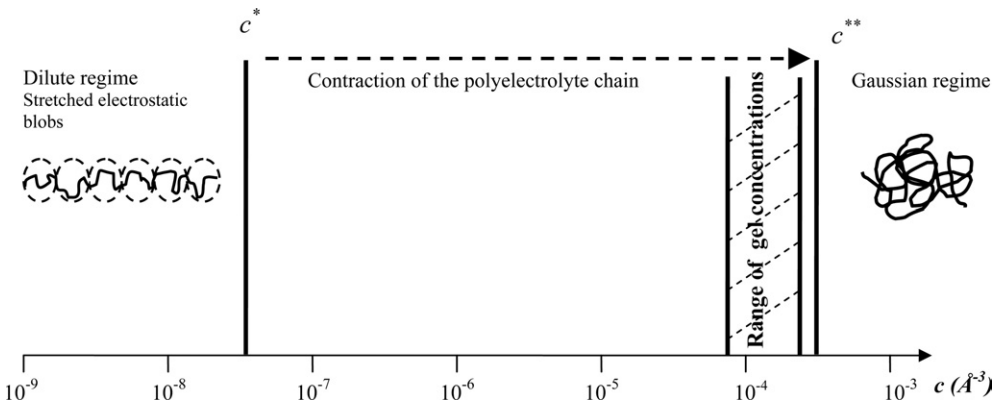

Fig. 7 Schematic representation of the conformation of polyelectrolyte chains as a function of concentration. Experimental gel concentrations used are also presented.

 This journal is © The Royal Society of Chemistry 2008

View Article Online

Published on 13 March 2008. Downloaded by Arts et Metiers Paris Tech on 29/06/2016 15:33:22.

discussion of the preceding paragraph and the comparisons between the purely Gaussian prediction and the polyelectrolyte ones, show that our gels should behave as Gaussian chains up to much larger values of λ than they do experimentally (see Fig. 4). This suggests the existence of another hardening mechanism active at relatively high strains and depending on the network structure since the decreasing trend of λ_{max} with increasing concentration is observed.

Hysteresis energy and inverse yielding effect

The second important point in the compression experiments presented in Fig. 4 was the significant hysteresis observed upon unloading and the fact that higher extensions resulted in larger observed hystereses.

The hysteresis, or energy dissipated during a loading/unloading cycle, is calculated according to the following equation:

$$E_{hyst} = \int_{loading} \sigma_{comp} d\varepsilon - \int_{unloading} \sigma_{comp} d\varepsilon \qquad (13)$$

with ε as defined before. This hysteresis was calculated for each sample of the three types of gels at increasing values of the maximum compressive force (the strain rate is kept constant $\approx 1.4 \times 10^{-2}$ s^{-1}). The results are presented in Fig. 8.

It appears in Fig. 8 that the hysteresis increases with maximum achieved strain in the loading step. Since the measured maximum extensibility depends on polymer concentration (Table 1), it is interesting to plot a normalized hysteresis energy *versus* a reduced lambda, defined as:

$$\lambda_{red} = \frac{\lambda_{biax} - 1}{\lambda_{biax,m} - 1},\ E_{norm} = \frac{E_{hyst}}{\int_{loading} \sigma_{comp} d\varepsilon} = 1 - \frac{\int_{unloading} \sigma_{comp} d\varepsilon}{\int_{loading} \sigma_{comp} d\varepsilon} \qquad (14)$$

where $\lambda_{biax,\,m}$ is the maximal biaxial lambda value obtained using the Gent fits ($\lambda_{biax,m} \approx \sqrt{\frac{J_m+3}{2}}$).

λ_{red} is 0 in the undeformed state and 1 when the extensibility is equal to its maximum value obtained using the Gent fits, and accounts for the concentration effects on the maximum extensibility (see Table 1). E_{norm} is equal to 0 when no significant hysteresis is measured and 1 when the stress falls back immediately to 0 when unloading starts.

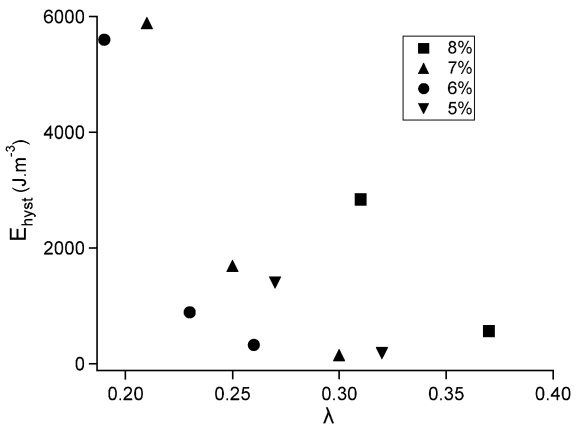

Fig. 8 Hysteresis energy as a function of lambda for several concentrations.

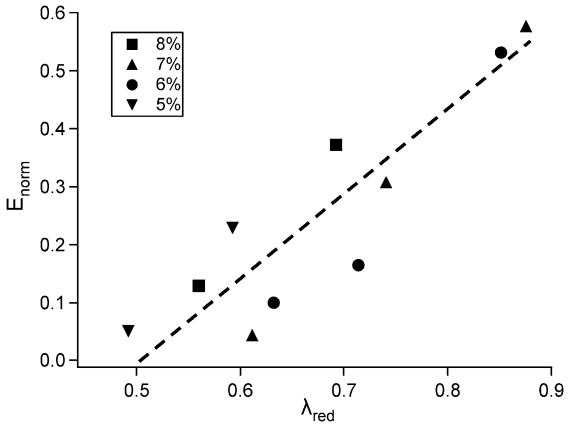

Fig. 9 Normalized hysteresis energy as a function of reduced lambda for several concentrations.

Although the data are noisy, it is clear from Fig. 9 that the hysteresis energy only appears at 50–60% of the maximum extensibility and increases subsequently (rather sharply) with increasing maximum strain. Since these hysteresis cycles are perfectly repeatable after a minute or so of holding time, this suggests a strain induced mechanism which is not immediately reversible. Further evidence toward such a mechanism is provided by careful analysis of the unloading curve. As shown in Fig. 10, the force drops rapidly when the strain is reversed and then unloading occurs at nearly constant force. Such an effect is reminiscent of what is observed for strain crystallisation of natural rubber in tension where the unloading occurs at constant force.[45] In the case of natural rubber unloading the effect has been attributed to progressive melting of the crystalline phase as the strain is reduced: as the crystallites melt, there is an equilibrium between two phases, amorphous and crystalline. When all the crystals have melted, the stress falls back to zero. This behaviour during unloading is close to the necking effect observed in amorphous and semi-crystalline materials and has been called the inverse yielding effect.[46,47]

In the case of our experiments on the hydrogels, it is clear that no crystallization can take place. However, this unloading under a constant force is reversible since a sample tested several times always has the same loading–unloading curve. These experiments would then be consistent with the hypothesis of a strain induced physical phenomenon responsible for the hardening during the loading phase and for the hysteresis and the stress plateau during the unloading. It is also noticeable that this plateau in force seems to depend on the maximum strain applied to the sample. For the 0.5 N test ($\lambda = 0.3$) the plateau is less pronounced while it is pronounced and identical for the 1 N and 5 N curves.

In order to test our hypothesis that the hysteresis was related to the aggregation of same charge polymer chains into bundles, we have performed several additional experiments.

Gels in NMP and in salt water

In order to investigate the effect of the presence of charges on the backbone chain, uncharged PAA gels in organic solvents (with

View Article Online

Published on 13 March 2008. Downloaded by Arts et Metiers Paris Tech on 29/06/2016 15:33:22.

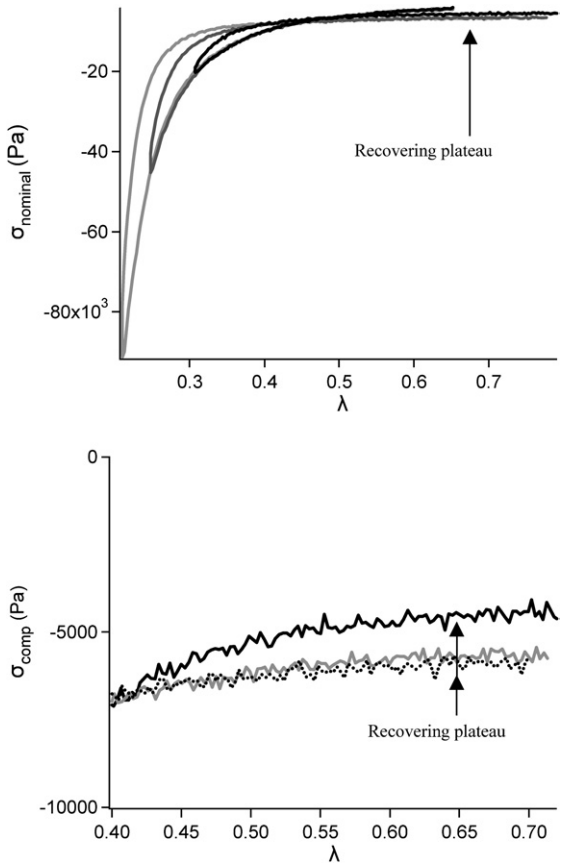

Fig. 10 Nominal stress *versus* deformation for a 6% PAA10db hydrogel at several maximum force values (black 0.5 N, light grey 1 N, dark grey 2 N) and zoom on the unloading curves at small deformations (black 0.5 N, light grey 1 N, dashed 5 N).

PAA chains under acidic form), were prepared as described earlier and the same experiments were performed on these gels swollen in NMP. Gels prepared in salt water were also studied, at low salt concentration (0.2 mol L^{-1}) with respect to the number of charges issued from the polymer backbone, and at high salt concentration (5 mol L^{-1}). Comparing the large strain behaviour of PAA10db gels in water, in the presence of salt (where charges inside the gel are screened), and in NMP (where the gel has to be swollen in its neutral form) will shed light on the role played by the charges in the abnormal large strain behaviour observed in pure water.

The results for the compression experiments are presented in Fig. 11. Samples roughly have the same dimensions (3.7 mm ± 0.1 in height, 2.7 mm in radius). The curves show the compressive stress *versus* λ to display the extensibility (a), the unloading plateau (b) and the hysteresis (c).

Two important points come out of these graphs. NMP-Gels have really different compression behaviours than the hydrogels. They deform with less hysteresis even at large strains, and the value of J_m is hard to obtain using the Gent fits, as the hardening has become very low (so have the hysteresis and the recovering plateau). However, the best fits give $J_m > 100$, which leads to $\lambda_{max,\ exp} > 10$, and these values are close to what is expected for a Gaussian network (see Table 1). Some further insights come from the experiments performed in salt water. When the

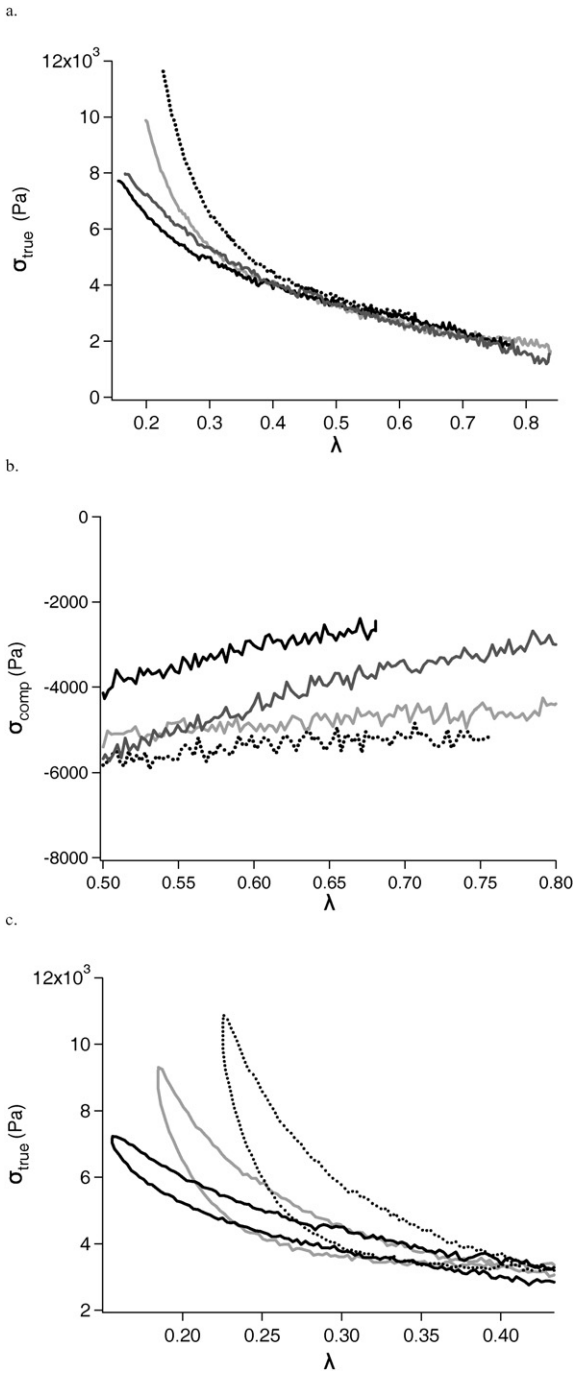

Fig. 11 (a) Effect of the charges on the hardening: true stress *versus* lambda for NMP 6% gels (black) and hydrogels at the same concentration (black dotted line). NaCl gels are the grey (0.2 mol L^{-1}) and dark grey curves (5 mol L^{-1}). (b) Effect of the charges on the recovery plateau: compressive stress *versus* lambda, same colours. (c) Effect of the charges on the hysteresis.

salt concentration is low (0.2 M), the stress–strain curve is similar to that obtained in pure water (strong strain hardening, large hysteresis and marked plateau during unloading) whereas at high salt concentrations (5 M) the hydrogel follows closely the stress–strain curve obtained for the gel in NMP. The electrostatic interactions between PAA chains are screened by the salt and the gel behaves almost like a neutral gel. This confirms that the early

 This journal is © The Royal Society of Chemistry 2008

View Article Online

Published on 13 March 2008. Downloaded by Arts et Metiers Paris Tech on 29/06/2016 15:33:22.

strain hardening and the hysteresis are clearly related to the presence of charges on the polyelectrolyte chains and not simply due to heterogeneities of the network.

Stress relaxation and strain rate effects: more insights in the dynamics of the aggregation process

Two types of experiment were performed comparatively on the gels in pure water, in salt water and in NMP in order to investigate the characteristic time scales of the relaxation process and its reversibility.

The graph presented in Fig. 12 shows the normalized true stress ($\sigma_{true}/\sigma_{true0}$ where σ_{true0} is the true stress at $t = 0$ which is the point when the maximum applied compression, *i.e.* the maximum deformation—*i.e.* the minimum lambda λ_{min}—is reached) as a function of time for different values of the maximum compressive strain for a PAA10db hydrogel at a concentration of 8%.

Apparently when $\lambda_{min} > 0.3$, little relaxation is observed and no obvious relaxation time is visible, whereas for lower λ_{min} two relaxation times are observed and the level of relaxation clearly increases (no significant differences are observed for the two curves at $\lambda_{min} = 0.2$ and $\lambda_{min} = 0.25$). The relaxation curves for $\lambda_{min} < 0.3$ can be fitted reasonably by a double exponential as shown in Fig. 13.

In consequence the system has two characteristic relaxation times. The first one is around 5–10s, whereas the second is very long, around 1500–2500 s and could be related to the life-time of the stiffening structure formed at high compressions. It is hard to propose a meaningful interpretation of the short characteristic time, since it is close to the duration of the compressive stage before the relaxation starts (see the experimental part).

Repeating the same experiments for several concentrations at increasing values of the maximum deformation applied, it is possible to determine approximately the critical deformation λ_c where two relaxation times are visible, as a function of concentration (see Table 2).

The results presented in Table 2 show that λ_c increases with concentration, which means that as the initial and isotropic charge concentration increases in the gel, the level of deformation where two relaxation times appear occurs for a lower level of strain (a higher λ_{min}). It is also noticeable that the ratio C/λ_c seems almost constant at $C/\lambda_c \approx 25$. This could be related to a critical normalized concentration, *i.e.* to a critical chain density (or charge density) in the compression direction at which the additional relaxation time appears.

When the relaxation experiments are performed on NMP gels and on gels prepared in salt water the results of the compression experiments are confirmed. It appears that there are no significant dissipative mechanisms in the NMP-gels (Fig. 14) even at very long times ($\sigma_{true}/\sigma_{true0} > 0.9$), regardless of the maximum deformation applied, while the gel prepared in a salt solution at low concentration has a relaxation behaviour close to that of the hydrogel in pure water. On the contrary the gel prepared at very high salt concentration behaves almost like the gel in NMP (Fig. 15). This is not a drying effect since it is not observed in every case (see for example NaCl 5 M gel in Fig. 15 where σ/σ_0

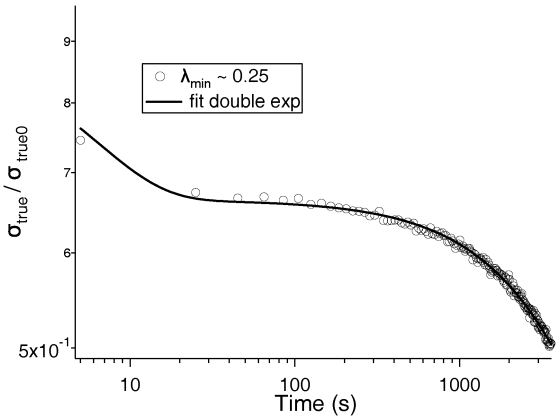

Fig. 13 Relaxation for a 10db6% hydrogel at $\lambda_{min} = 0.2$ and the fit with a double exponential function.

Table 2 Critical compressive lambda λ_c for PAA10db at several concentrations

C(%)	5%	6%	8%
λ_c	0.2 ± 0.025	0.25 ± 0.025	0.3 ± 0.025

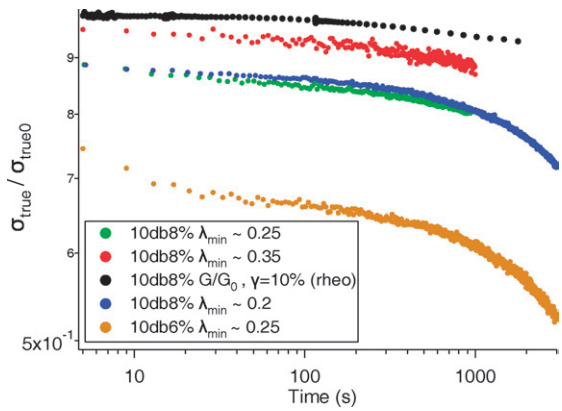

Fig. 12 Relaxation experiments: normalized true stress over time for a 10db6% hydrogel and a 10db8% hydrogel compressed at different maximum strains.

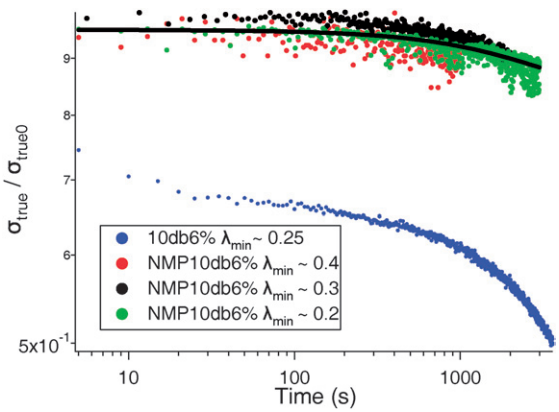

Fig. 14 NMP gel relaxation compared to the hydrogel relaxation.

View Article Online

Published on 13 March 2008. Downloaded by Arts et Metiers Paris Tech on 29/06/2016 15:33:22.

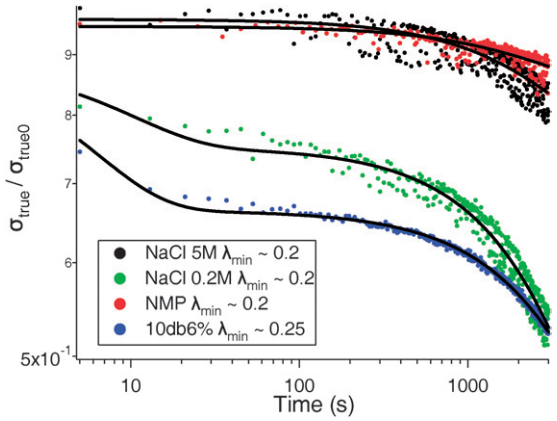

Fig. 15 NaCl gel relaxation compared to NMP gel and hydrogel relaxation at 6%.

falls only from 0.92 to 0.89 between 1000 and 3000 s, while it falls from 0.62 to 0.52 during the same time for the 10db hydrogel—see also the drying experiments presented before).

Since the stress relaxes with two distinct time scales, it is interesting to study the strain rate effects on the compression experiments. According to Fig. 13, the plateau in relaxation is located between 20 and 700 s. In this range of times, the stress is almost unchanged. But for experiments shorter than 10 s, and for experiments longer than 1000 s, one expects to see some differences in the stress–strain curves, since σ/σ_0 is roughly 0.75 after 5 s but only 0.55 after 2000 s (10db 6% hydrogel). At very long times, if drying of the sample can be avoided, one can expect the polymer chains to rearrange to a more homogeneous distribution of charges and tend toward the behaviour of the uncharged gel.

In consequence, samples of the same material at the same gel concentration were compared at different crosshead velocities, varying from 1 μm s^{-1} to 600 μm s^{-1} corresponding to initial strain rates of $\dot{\varepsilon}$ varying from 3×10^{-4} to 0.17 s^{-1}. The total time of the experiment varied from 3600 s to 5 s. Results are presented in Fig. 16 for 6% hydrogels.

Fig. 16 shows clearly a rate dependence of the stress–strain behaviour, as it was predicted by the relaxation experiments discussed above. For low strain rates, the strain hardening and the hysteresis diminish.

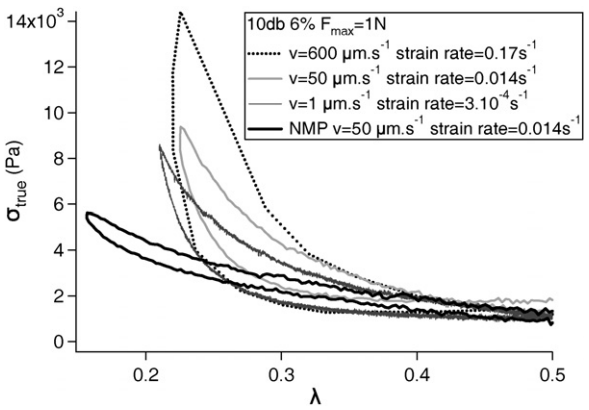

Fig. 16 Strain rate effects on the stress–strain behaviour for 6% hydrogels at several strain rates.

Using the Gent fits for the loading curves, the maximal values of lambda ($\lambda_{max,\ exp}$) were obtained for the different initial strain rates and show a slight increase with decreasing strain rate: $\lambda_{max,\ exp} = 3.6$, 3.4 and 3.3 were found for compressions performed at 3×10^{-4}, 0.014 and 0.17 s^{-1} respectively (force applied: 1 N—note that the maximal force applied affects slightly the results of the Gent fits, as discussed in the strain hardening section; this explains the small differences between these values and those discussed earlier) whereas a value of 10 can be estimated for the NMP gels. These results indicate a strain rate effect on the strain hardening and hysteresis mechanisms.

Coming back to Fig. 13, it is possible to estimate the extent of stress relaxation for a 5 s experiment ($\dot{\varepsilon} = 0.17\ s^{-1}$), $\sigma_{true}/\sigma_{true0} = 0.75$, whereas for a 3600 s experiment ($\dot{\varepsilon} = 3 \times 10^{-4}\ s^{-1}$), $\sigma_{true}/\sigma_{true0} = 0.5$. The two values of maximal stress upon loading obtained at these initial strain rates for the loading–unloading experiments are 14 kPa and 9 kPa for 600 μm s^{-1} and 1 μm s^{-1} respectively. The ratio $14/9 \approx 1.5$ is close to the relaxation ratio $0.7/0.5 = 1.4$.

Discussion

One of the striking results of our study is the large difference between the observed finite extensibilities of the chains and the theoretical values. This result could be due to a high level of heterogeneities in the network (high polydispersity of N_c and/or dangling chains): this could lead to a percolating structure of short chains and in that case the experimental limiting extensibility would be controlled by the short chain population rather than the long ones, and the result would be a lower λ_{max} than the theoretical one obtained for a homogeneous value of N_c. However the important hysteresis and the fact that the strain hardening disappears when the exact same gel sample is swollen in an organic solvent suggests that this is not due to a heterogeneity effect (such a phenomenon should be mostly reversible and solvent independent).

Additionally, the results obtained for the gels prepared in salt water, where the hysteresis, stress plateau and hardening are much less pronounced (and decrease with increasing salt concentration, *i.e.* as the electrostatic interactions are screened), show that the charges along the backbone play a major role in the non Gaussian behavior observed at large strains on these polyelectrolyte hydrogels.

If we observe the stress–strain curves (Fig. 4 and Fig. 10) as well as the velocity dependence in Fig. 16 it is clear that the material behaves as if its stiffness progressively increased and then decreased with a time lag. The question is then, what causes this increase in stiffness which has some stability in time but disappears completely when the material is fully unstressed. We explored several hypotheses and will now discuss what we think is the most likely one based on theoretical arguments and previous results: the formation of clusters between chains of the same charge.

Let us make the hypothesis that the presence of charges on the chain creates clustering (bundles). We can make a simple calculation based on the Oosawa's model[11] presented in the introduction. Oosawa predicted that the attraction between two charged chains should occur for distances smaller than $l_b(m/m^* - 1)^2$ where l_b is the Bjerrum length, m is the fraction of charged real

 This journal is © The Royal Society of Chemistry 2008

View Article Online

Published on 13 March 2008. Downloaded by Arts et Metiers Paris Tech on 29/06/2016 15:33:22.

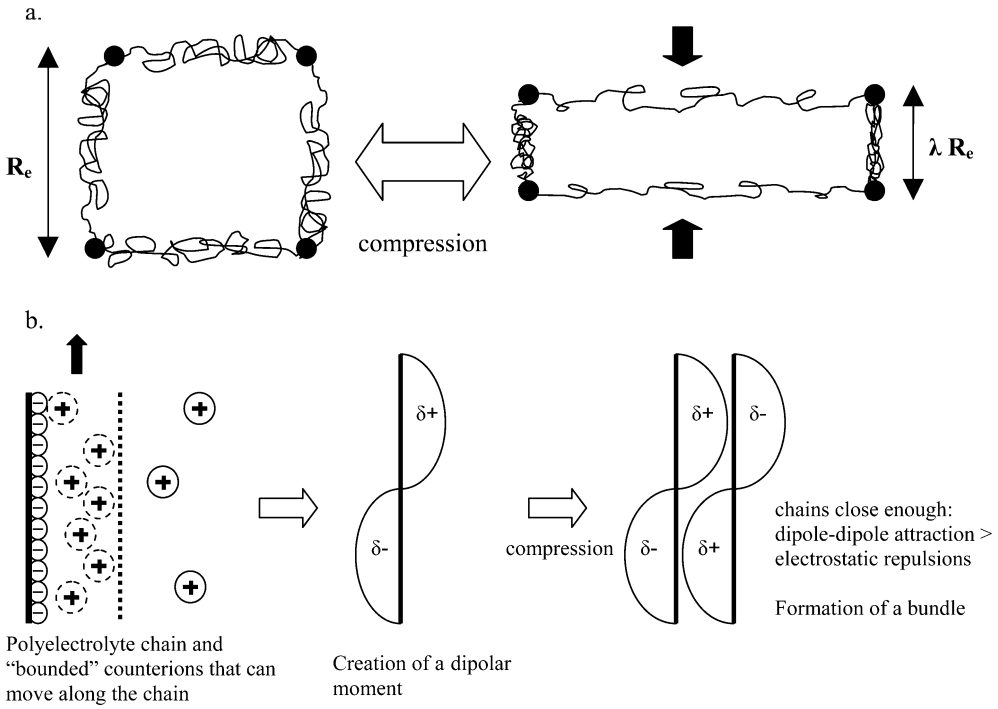

Fig. 17 Simple schematic for the estimate of the distance between chains (a) in the compression direction and the resulting aggregation (b).

monomers and m^* is the effective fraction of charged real monomers (see ESI†). For our systems this gives roughly $3.5l_b \approx 25$ Å.

If we assume that the network is homogeneously crosslinked, the distance between two strands is R_e (eqn (11)). When the network is compressed, considering an affine deformation, we can simply estimate that, in the 1-direction (*i.e.* in the compression direction), the distance between two chains becomes λR_e, with λ the macroscopic deformation (see Fig. 17).

We can estimate, by using the results presented before for R_e, the critical distance between two chains in the 1-direction at the critical deformation λ_c presented in Table 2. We obtain (considering that the experimental λ_c is given with an error of about ± 0.025) a constant value, independent of the concentration and of the mesh size of the network, $d \approx 35$ Å. This value is quite close, although a bit larger, to the simple prediction by Oosawa. However, in this oversimplified calculation, the mesh size distribution is not taken into account. The scheme presented in Fig. 17 also represents a 2 chain aggregation whereas in solutions the typical size of a polyelectrolyte bundle was estimated to be close to 1000 Å (with our calculation, roughly 30 chains).

The results presented also suggest a continuous transition rather than an abrupt one: it seems that aggregates are created all across the network till they form a "percolating" structure which then begins to affect the macroscopic properties of the gel. This progressively percolating structure is responsible for the increase in stiffness and progressively traps elastic chains between stiffer connected structures as shown schematically in Fig. 18.

Another interesting feature of the phenomenon is its dynamics. As long as the macroscopic deformation is maintained, the high stiffness is relatively stable. Stress only relaxes over rather long times and we have no evidence that the structure responsible for the higher stiffness disappears; it could simply rearrange. However when the deformation is removed the high stiffness disappears completely over times that are much shorter (consecutive experiments after 100 s waiting times are fully reproducible). These results are confirmed by compressions made at very low speeds, which seem to indicate that the gel is less and less sensitive to the ionic effects if a very low compression rate is applied. At very long times, if drying could be avoided, one can expect to obtain the same behaviour for the polyelectrolyte gels as for the NMP gels. This behaviour is completely different from for example the crystallisation in natural rubbers which is a thermodynamically stable process, *i.e.* if the deformation is maintained, the crystals are permanent. If they exist, the ionic associations between chains seem here to be a dynamic process. The size and/or the number of clusters will be rate dependent and the system reorganizes over time, relaxing energy during this process.

A very puzzling result is the crossing of the loading and unloading curves at low deformations, which is apparent in Fig. 10. At values of $\lambda > 0.5$, the unloading curve is higher then the loading curve. In other word there is more elastic energy stored during unloading that during loading. This suggests the existence of a mechanism to trap elastic energy and release it with a time lag. The proposed mechanism is described schematically in Fig. 18.

An important question which we have to address is the possible origin of the aggregation. Some studies have shown that hydrophobic chain ends could significantly modify the same charge attraction between polyelectrolytes.[8] To convince ourselves that the thiol–ene chemistry used for crosslinking the gel was not the reason for the aggregation we carried out some complementary experiments on a PAA hydrogel synthesised by a simple radical reaction (crosslinker: *N*,*N*′-methylenebisacrylamide, redox: KPS and *N*,*N*,*N*′*N*′-tetramethylethylenediamine) and they showed qualitatively the same effects, suggesting that

View Article Online

Published on 13 March 2008. Downloaded by Arts et Metiers Paris Tech on 29/06/2016 15:33:22.

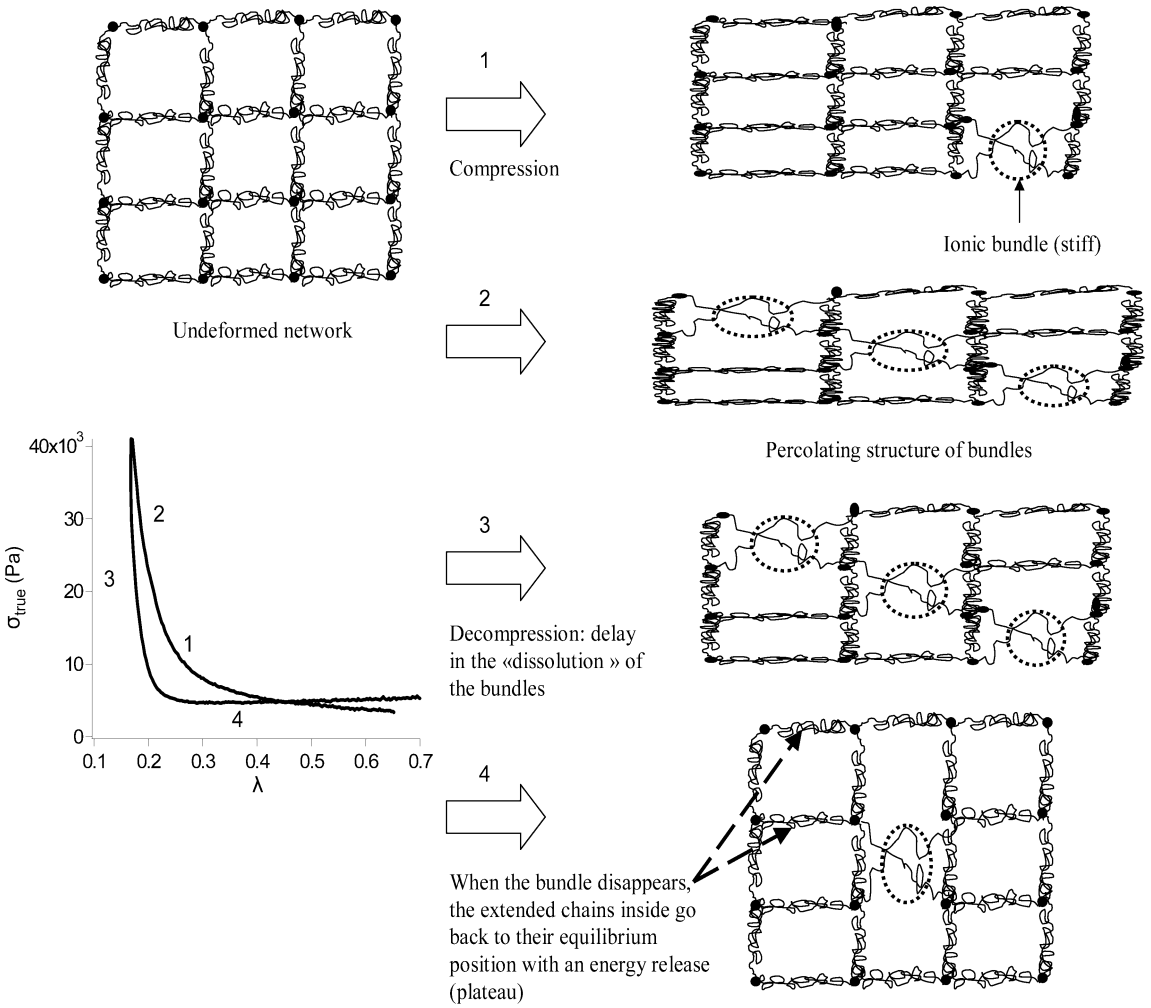

Fig. 18 Schematic of the proposed formation and dissolution of the bundled structure. 1–2) During the compression, progressive formation of ionic bundles which stiffen the structure. As the bundle structure percolates the Gaussian chains are trapped in various states of extension between stiffer structures. 3–4) During unloading the bundles progressively dissolve, freeing therefore the elastic chains which release their elastic energy with a delay. On the left, the corresponding regions on a loading–unloading curve.

this dynamic strain-induced ionic aggregation in highly charged polyelectrolyte hydrogels may be a general phenomenon.

Of course we did not perform any scattering experiments on our gels under strain to prove the existence of these structural changes occurring during deformation. However, one should keep in mind that the phenomena observed are dynamic with a life-time (roughly 2000 s) that is quite short compared to the times needed in neutron scattering, for example. In consequence, the structures in the gel will probably change with a time shorter than the experimental time.

In conclusion, although we do not have a direct proof that these ionic bundles exist or what their shape or structure actually is, we have strong concurring evidence that our model of ionic aggregation is plausible and could potentially be general.

Conclusion

In this article, we demonstrated for the first time an unexpected behaviour that could potentially be general for highly charged polyelectrolyte hydrogels undergoing large strain compressions.

Important strain hardening, high hysteresis and a stress plateau during unloading were clearly observed. These phenomena are time- and strain-dependant: and were not observed for gels deionised after gelation (NMP gels). They are also significantly less pronounced when the backbone charges were screened in the presence of salt. We proposed that these effects are due to a mechanism of reversible strain induced polyelectrolyte associations due to attractive forces between identically charged polyions in hydrogels. These associations form progressively a stiffer percolating structure which can then be dissolved with a time lag during unloading.

If this mechanism is correct it would demonstrate that, for polyelectrolyte hydrogels, *i.e.* materials which cannot flow, applying a strong external constraint (compression) can lead to the same chain aggregation effects as when the polymer concentration is increased or the Bjerrum length is increased (by changing the solvent or increasing the valence of the counterion).[3]

It would also show that these associations can occur in the presence of monovalent cations (Na^+), as observed and predicted theoretically in polyelectrolyte solutions,[6,14,16,17] so the valence of

 This journal is © The Royal Society of Chemistry 2008

View Article Online

the counterions is not the only relevant parameter to describe this phenomenon.

Acknowledgements

We would like to thank J.F. Joanny and H.R. Brown for interesting discussions on polyelectrolyte and mechanical results, and for great experimental suggestions. We would also like to thank Trisan Baumberger for his critical reading of the manuscript and helpful suggestions.

References

1 A. Katchalsky, S. Lifson and J. Mazur, *J. Polym. Sci.*, 1953, **11**(5), 409.
2 A. Y. Grosberg, T. T. Nguyen and B. I. Shklovskii, *Rev. Mod. Phys.*, 2002, **74**(2), 329.
3 J. L. Barrat and J. F. Joanny, *Adv. Chem. Phys.*, 1996, **94**(1), 1.
4 S. M. Klimenko, T. I. Tikchonenko and V. M. Andreev, *J. Mol. Biol.*, 1967, **23**(3), 523.
5 V. A. Bloomfield, *Biopolymers*, 1991, **31**(13), 1471.
6 Y. Zhang, J. F. Douglas, B. D. Ermi and E. J. Amis, *J. Chem. Phys.*, 2001, **114**(7), 3299.
7 J. J. Tanahatoe and M. E. Kuil, *J. Phys. Chem. B*, 1997, **101**(45), 9233.
8 B. Hammouda, F. Horkay and M. L. Becker, *Macromolecules*, 2005, **38**, 2019.
9 P. Wissenburg, T. Odijk, P. Cirkel and M. Mandel, *Macromolecules*, 1995, **28**, 2315.
10 B. D. Ermi and E. J. Amis, *Macromolecules*, 1998, **31**, 7378.
11 F. Oosawa, *Polyelectrolytes*, Dekker, New York, 1971.
12 G. S. Manning, *J. Chem. Phys.*, 1969, **51**, 954.
13 B. I. Shklovskii, *Phys. Rev. Lett.*, 2000, **82**(16), 3268.
14 J. Ray and G. S. Manning, *Macromolecules*, 2000, **33**, 2901.
15 M. L. Henle and P. A. Pincus, *Phys. Rev. E*, 2005, **71**(6), 060801, part 1.
16 T. B. Liverpool and K. K. Müller-Nedebock, *J. Phys.: Condens. Matter*, 2006, **18**, L135.
17 F. Horkay, A. M. Hecht, P. J. Basser and E. Geissler, *Macromolecules*, 2001, **34**, 4285.
18 R. Skouri, F. Schosseler, J. P. Munch and S. J. Candau, *Macromolecules*, 1995, **28**, 197.
19 O. Okay, S. B. Sariisik and S. D. Zor, *J. Appl. Polym. Sci.*, 1998, **70**, 567.
20 E. Jabbari and S. Nozari, *Eur. Polym. J.*, 2000, **36**(12), 2685.
21 G. Nisato, R. Skouri, F. Schosseler, J. P. Munch and S. J. Candau, *Faraday Discuss.*, 1995, **101**, 133.
22 N. Gundogan, D. Melekaslan and O. Okay, *Eur. Polym. J.*, 2003, **39**(11), 2209.
23 M. Rubinstein, R. H. Colby, A. V. Dobrynin and J. F. Joanny, *Macromolecules*, 1996, **29**(1), 398.
24 A. R. Khokhlov and E. Y. Kramarenko, *Macromolecules*, 1996, **29**, 681.
25 V. A. Smirnov, G. A. Sukhadolski, O. E. Philippova and A. R. Khokhlov, *J. Phys. Chem. B*, 1999, **103**(36), 7621.
26 T. Minato and M. Satoh, *J. Polym. Sci., Part B*, 2004, **42**(23), 4412.
27 *Hydrogels in Medicine and Pharmacy*, ed. N. A. Peppas, CRC Press Inc, Boca Raton, FL, 1986, vol. 1 and 2.
28 H. J. Kwon, Y. Osada and J. P. Gong, *Polym. J.*, 2006, **38**(12), 1211.
29 A. H. Clark and S. B. Ross-Murphy, *Adv. Polym. Sci.*, 1987, **83**, 57.
30 J. P. Gong, Y. Katsuyama, T. Kurokawa and Y. Osada, *Adv. Mater.*, 2003, **15**(14), 1155.
31 K. Haraguchi and H. J. Li, *Macromolecules*, 2006, **39**, 1898.
32 R. E. Webber, C. Creton, H. R. Brown and J. P. Gong, *Macromolecules*, 2007, **40**, 2919.
33 T. Baumberger, C. Caroli and D. Martina, *Eur. Phys. J. E*, 2006, **21**(1), 81.
34 G. Miquelard-Garnier, S. Demoures, C. Creton and D. Hourdet, *Macromolecules*, 2006, **39**, 8128.
35 G. Josse, P. Sergot, M. Dorget, C. Creton and M. Dorget, *J. Adhes.*, 2004, **80**, 87.
36 A. N. Gent, *Rubber Chem. Technol.*, 1996, **69**, 59.
37 A. N. Gent, *J. Rheol.*, 2005, **49**(1), 271.
38 C. O. Horgan and J. G. Schwartz, *J. Mech. Phys. Solids*, 2005, **53**, 545.
39 R. A. Dickie and T. L. Smith, *J. Polym. Sci., Part A*, 1969, **7**, 687.
40 M. C. Boyce and E. M. Arruda, *Rubber Chem. Technol.*, 2000, **73**, 504.
41 L. R. G. Treloar, *The Physics of Rubber Elasticity*, Clarendon Press, Oxford, 3rd edn, 1975.
42 A. V. Dobrynin and M. Rubinstein, *Prog. Polym. Sci.*, 2005, **30**, 1049.
43 T. J. Taylor and S. S. Stivala, *Polymer*, 1996, **37**(5), 715.
44 A. Takahashi and M. Nogasawa, *J. Am. Chem. Soc.*, 1964, **86**(4), 543.
45 P. A. Albouy, J. Marchal and J. Rault, *Eur. Phys. J. E*, 2005, **17**, 247.
46 S. Toki, I. Sics, S. Ran, L. Liu, B. S. Hsiao, S. Murakami, K. Senoo and S. Kohjiya, *Macromolecules*, 2002, **35**, 6573.
47 S. Trabelsi, P. A. Albouy and J. Rault, *Macromolecules*, 2003, **36**, 6462.

Published on 13 March 2008. Downloaded by Arts et Metiers Paris Tech on 29/06/2016 15:33:22.